Nuclear Engineering and Technology 56 (2024) 1562–1573

Contents lists available at ScienceDirect

Nuclear Engineering and Technology

journal homepage: www.elsevier.com/locate/net

Original Article

Uncertainty analysis of UAM TMI-1 benchmark by STREAM/RAST-K

Jaerim Jang [a], Yunki Jo [b], Deokjung Lee [b,c,*]

[a] Advanced Reactor Technology Development Division, Korea Atomic Energy Research Institute, Daedeok-daero 989-111, Yuseong-gu, Daejeon, 305-335, Republic of Korea
[b] Department of Nuclear Engineering, Ulsan National Institute of Science and Technology, 50 UNIST-gil, Eonyang-eup, Ulju-gun, Ulsan, 44919, Republic of Korea
[c] Advanced Nuclear Technology and Services, 406-21 Jonga-ro, Jung-gu, Ulsan, 44429, Republic of Korea

ARTICLE INFO

Keywords:
PWR
UAM benchmark
TMI-1
Uncertainty quantification
Two-step method

ABSTRACT

This study rigorously examined uncertainty in the TMI-1 benchmark within the Uncertainty Analysis in Modeling (UAM) benchmark suite using the STREAM/RAST-K two-step method. It presents two pivotal advancements in computational techniques: (1) Development of an uncertainty quantification (UQ) module and a specialized library for the pin-based pointwise energy slowing-down method (PSM), and (2) Application of Principal Component Analysis (PCA) for UQ. To evaluate the new computational framework, we conducted verification tests using SCALE 6.2.2. Results demonstrated that STREAM's performance closely matched SCALE 6.2.2, with a negligible uncertainty discrepancy of ±0.0078% in TMI-1 pin cell calculations. To assess the reliability of the PSM covariance library, we performed verification tests, comparing calculations with Calvik's two-term rational approximation (EQ 2-term) covariance library. These calculations included both pin-based and fuel assembly (FA-wise) computations, encompassing hot zero-power and hot full-power operational conditions. The uncertainties calculated using both the EQ 2-term and PSM resonance treatments were consistent, showing a deviation within ±0.054%. Additionally, the data compression process yielded compression ratios of 88.210% and 92.926% for on-the-fly and data-saving approaches, respectively, in TMI fuel assembly calculations. In summary, this study provides a comprehensive explanation of the PCA process used for UQ calculations and offers valuable insights into the robustness and reliability of newly developed computational methods, supported by rigorous verification tests.

1. Introduction

This paper conducts a comprehensive uncertainty analysis of the TMI-1 benchmark, a component of the Uncertainty Analysis in Modeling (UAM) benchmark suite, utilizing the STREAM/RAST-K two-step method [1–3]. This study introduces two significant innovations: (1) the generation of a covariance library tailored for the pin-based pointwise energy slowing-down method (PSM) [4], and (2) the integration of Principal Component Analysis (PCA) for Uncertainty Quantification (UQ) [5,6]. To validate these advancements, we undertook various verification exercises using SCALE 6.2.2 as a reference and leveraged its covariance library [7]. To obtain a more holistic solution, this study further incorporates ENDF/B-VII.1 covariance data [8].

UQ is pivotal in a range of applications, such as safety analysis, licensing procedures, and design development. For example, the UQ plays a critical role in defining safety criteria, such as the upper safety limit in burnup credit calculations, which in turn influences the design of spent nuclear fuel casks and pools [9]. Additionally, the UQ helps establish confidence intervals in transient safety analyses such as rod ejection scenarios. This work aligns with broader initiatives, such as the UAM benchmark developed by the Expert Group on Uncertainty Analysis in Modeling (EGUAM) under the aegis of the Working Party on Scientific Issues in Reactor Systems (WPRS). The UAM benchmark aims to quantify the modeling uncertainties in reactor systems under both steady-state and transient conditions [1].

In this study, with an aim to offer compatible solutions for the UAM benchmark, we employed the Method of Characteristics (MOC) code STREAM and a two-step code system, STREAM/RAST-K. This initiative involved participation of 19 computational codes across 15 countries [1]. To keep pace with these developments, we have designed an in-house UQ calculation module [9,10]. The effectiveness of this module was substantiated through verification against the UAM benchmark and

* Corresponding author. Department of Nuclear Engineering, Ulsan National Institute of Science and Technology, 50 UNIST-gil, Eonyang-eup, Ulju-gun, Ulsan, 44919, Republic of Korea.
E-mail address: deokjung@unist.ac.kr (D. Lee).

https://doi.org/10.1016/j.net.2023.12.010
Received 13 September 2023; Received in revised form 26 November 2023; Accepted 2 December 2023
Available online 8 December 2023

Table 1
Reaction list used in perturbation with 72G and 10,000G.

1. EQ 2-term					
Index	Reaction	MT	Index	Reaction	MT
1	Elastic scattering cross section	2	8	Production of a deuteron	104
2	Inelastic scattering cross section	4	9	Production of a triton	105
3	Fission cross section	18	10	Production of an alpha particle	107
4	Capture cross section	102	11	Production of a triton and 2 alpha particles	113
5	Production of two neutrons	16	12	Average number of prompt neutrons released per fission event	456
6	Production of three neutrons	17	13	Average number of delayed neutrons released per fission event	455
7	Production of a proton	103	14	Fission spectrum reactions	LF 18
2. PSM					
1	Fission cross section	18	2	Capture cross section	102
3	Total cross section	1			

comparison with the results generated using SCALE 6.2.2.

Furthermore, we discuss data compression techniques using PCA because efficient data management is vital in computational processes, particularly for memory optimization [5,6]. PCA offers several advantages over other compression methods such as xz, including memory conservation and the ability to use direct data [11]. In neutronic physics, PCA has been applied to compress a variety of datasets such as pin-by-pin burnup information and perturbed neutronics data, as shown in previous studies [5,12,13]. The novelty of this study lies in the direct application of the compressed data for both calculations and data storage. Previous research indicated that PCA can achieve truncation errors within 0.01% and a compression ratio exceeding 90% [5], reinforcing its applicability and efficiency in the UQ context.

The remainder of this paper is organized as follows: Section 2 offers an exhaustive description of the calculation procedures, the generated PSM covariance library, and the application of PCA in the two-step method. Section 3 outlines the criteria used in the UAM benchmark for validation. Section 4 presents a detailed analysis of the UAM benchmark results, contrasting the computational capabilities of STREAM with those of both the PSM and Calvik's two-term rational approximation [14–16] (EQ 2-term) covariance libraries. This section elaborates on PCA-based calculations.

2. Code system

In this study, UQ was executed using STREAM and STREAM/RAST-K two-step methods. Within the STREAM framework, perturbations were introduced into neutronics data. During the STREAM/RAST-K two-step computation, STREAM generates few-group constants based on perturbed cross-sectional data, which RAST-K then uses for 3D core simulations. This two-step approach has undergone rigorous verification and validation in commercial reactors, including the OPR-1000, APR-1400, and Westinghouse 3-loop reactors [17].

Perturbation of the neutronics data occurs between the cross-

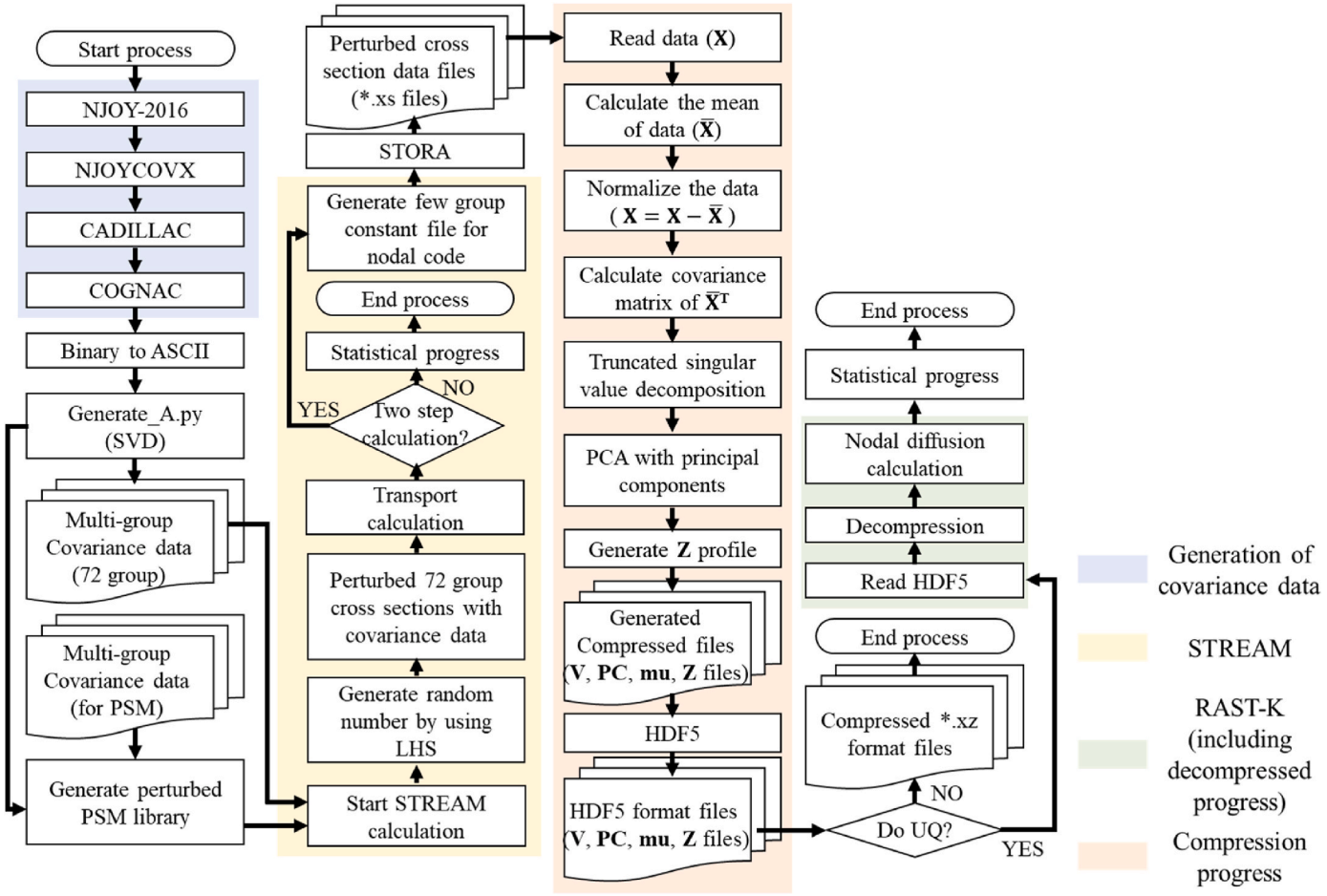

Fig. 1. Flow chart of perturbed data.

Table 2
Isotope list perturbed by ENDF/B-VII.1 covariance data.

^{1} and ^{2}H, ^{4}He, ^{6} and ^{7}Li, ^{9}Be, ^{10} and ^{11}B, C, ^{15}N, ^{16}O, ^{19}F, ^{23}Na, ^{24}Mg, ^{27}Al, $^{28-29}$, and ^{30}Si, ^{41}K, $^{46-50}$Ti, $^{50-52}$, and ^{53}Cr, ^{55}Mn, $^{54-56}$, and ^{57}Fe, ^{59}Co, ^{58} and ^{60}Ni, ^{89}Y, $^{90-96}$Zr, ^{95}Nb, $^{92, 94-100}$Mo, ^{99}Tc, $^{101-104,106}$Ru, ^{103}Rh, $^{105-108}$Pd, ^{109}Ag, ^{127,129}I, $^{131-132,134}$Xe, ^{133} and ^{135}Cs, ^{139}La, ^{141}Ce, ^{141}Pr, $^{143-145-146}$, and ^{148}Nd, ^{147}Pm, $^{149-151,152}$Sm, ^{153,155}Eu, $^{152-160}$Gd, $^{166-168,170}$Er, ^{169}Tm, $^{180-182-184}$, ^{186}W, ^{191,193}Ir, ^{197}Ag, $^{204,206-209}$Pb, ^{209}Bi, $^{227-234}$Ac, $^{229-230}$, ^{232}Pa, $^{230-233-234-235-236}$, ^{238}U, $^{234-239}$Np, $^{236-240-241}$, $^{242-246}$Pu, $^{240-241-242-242m}$, ^{243}Am, $^{240-250}$Cm, $^{245-250}$Bk, ^{246}, $^{248-254}$Cf, $^{251-255}$, ^{254m}Es, ^{255}Fm.

sectional data retrieval and resonance treatment steps within STREAM. In earlier versions of the UQ module, the resonance treatment supported only EQ 2-term method due of the absence of a PSM covariance library. However, previous research makes it evident that Ref. [4], PSM provides superior accuracy compared with EQ 2-term approach. To augment the computational precision of the lattice code calculations and expand the utility of the developed UQ module, we introduced a covariance library and a perturbation module specifically designed for PSM. The NJOY-2016 code [18] was used to generate a library based on the ENDF/B-VII.1 database [8]. To generate covariance libraries, we utilized both a 72-energy group structure and 10,000-energy group structure. EQ 2-term covariance library relies on a 72-energy group structure for 14 different neutronic reactions, as listed in Table 1. The categorization of MT and LF complied with the ENDF-6 manual [19]. During the perturbation analysis, the study does not consider the correlated effects between different isotopes, such as the relationship between ^{235}U (ν) and ^{238}U (ν).

EQ 2-term approach incorporates equivalence theory and Carlvik's two-term rational approximation [14,15]. The term "2-term" refers to the utilization of Carlvik's two terms to determine the Dancoff factor, as outlined in the literature [15,16]. Conversely, PSM employs a pin-based pointwise slowing-down methodology for resonance treatment, with the core idea centered on subdivided isolated fuel pins. Implementing the PSM involves a three-step procedure to approximate the collision probabilities: (1) The collision probability from points *i* and j within the subdivided isolated fuel pin is calculated using the Collision Probability Method solver [4]; (2) The Dancoff factor is determined through Carlvik's two-term rational approximation and the neutron-enhanced neutron current method [4], which also yields the shadowing effect correction factor. This factor represents the ratio of fuel escape probabilities between an isolated fuel pin and a pin within a lattice; (3) This shadowing effect correction is subsequently applied, resulting in adjusted escape and collision probabilities.

2.1. Stochastic sampling method

The STREAM/RAST-K two-step method features an UQ module designed using a stochastic sampling technique, as illustrated in Fig. 1. Perturbation analysis is performed with covariance library generated by NJOY-2016. Following NJOY calculations, the processed data were further refined using this covariance library. Various computational tools, including NJOYCOVX [20], CADILLAC [7], and COGNAC [7] have been employed for these calculations, as demonstrated in a previous study [16]. For the perturbation analysis, singular value decomposition (SVD) was applied to 182 isotopes by using Equations (1) and (2). Detail isotope list is illustrated in Table 2 [9,10]. Equations (1) and (2) are for perturbation analysis with 72-energy group structure and 10,000-energy group structure, respectively. The matrix sizes of Equations (1) and (2) are defined as 1,008 by 1,008 and 30,000 by 30,000, respectively. Here, 1,008 is determined by multiplying 72 (the number of energy groups) by 14 (the number of reactions considered in uncertainty quantification). These isotopes were selected from the ENDF/B-VII.1 covariance library, a list also referenced in previous studies [9,10,16].

$$\mathbf{C}=\begin{bmatrix} c_{1,1} & c_{1,2} & \cdots & c_{1,11} & \mathbf{O} & \mathbf{O} & \mathbf{O} \\ c_{1,2}^{T} & c_{2,2} & \vdots & \vdots & \vdots & \vdots & \vdots \\ \vdots & \cdots & \ddots & c_{10,11} & \mathbf{O} & \mathbf{O} & \mathbf{O} \\ c_{1,11}^{T} & \cdots & c_{10,11}^{T} & c_{11,11} & \mathbf{O} & \mathbf{O} & \mathbf{O} \\ \mathbf{O} & \cdots & \mathbf{O} & \mathbf{O} & \overline{\nu}_{p} & \mathbf{O} & \mathbf{O} \\ \mathbf{O} & \cdots & \mathbf{O} & \mathbf{O} & \mathbf{O} & \overline{\nu}_{d} & \mathbf{O} \\ \mathbf{O} & \cdots & \mathbf{O} & \mathbf{O} & \mathbf{O} & \mathbf{O} & \chi \end{bmatrix} \tag{1}$$

$$\mathbf{C_{PSM}}=\begin{bmatrix} c_{PSM,1,1} & c_{PSM,1,2} & c_{PSM,1,3} \\ c_{PSM,1,2}^{T} & c_{PSM,2,2} & c_{PSM,2,3} \\ c_{PSM,1,3}^{T} & c_{PSM,2,3}^{T} & c_{PSM,3,3} \end{bmatrix} \tag{2}$$

where **O** is a zero matrix of size 72 × 72. The matrices of **C** and $\mathbf{C_{PSM}}$ are covariance matrices for EQ 2-term and PSM methods, respectively. The notation of c_{I_1,I_2} and c_{PSM,I_1,I_2} are the covariance data matrices among I_1 cross section and I_2 cross-sections and is a 72 × 72 size matrix and 10,000 × 10,000 size matrix. The formats of I_1 and I_2 are generated using *X*. Notation *X* corresponds to the reaction indices presented in Table 1. By applying the singular value decomposition relationship, the covariance matrix can be defined as shown in Equation (3). Equation (4) is utilized for the perturbation of cross-section data.

$$\begin{cases} \boldsymbol{C}=\boldsymbol{U\Sigma U}^{\boldsymbol{T}}=\boldsymbol{AA}^{\boldsymbol{T}}\ (\text{EQ 2}-\text{term}) \\ \boldsymbol{C}_{\boldsymbol{PSM}}=\boldsymbol{U}_{\boldsymbol{PSM}}\boldsymbol{\Sigma}_{\boldsymbol{PSM}}\boldsymbol{U}_{\boldsymbol{PSM}}^{\boldsymbol{T}}=\boldsymbol{A}_{\boldsymbol{PSM}}\boldsymbol{A}_{\boldsymbol{PSM}}^{\boldsymbol{T}}\ (\text{PSM}) \end{cases} \tag{3}$$

$$\begin{cases} \boldsymbol{A}=\boldsymbol{U}\sqrt{\boldsymbol{\Sigma}}\ (\text{EQ 2}-\text{term}) \\ \boldsymbol{A}_{\boldsymbol{PSM}}=\boldsymbol{U}_{\boldsymbol{PSM}}\sqrt{\boldsymbol{\Sigma}_{\boldsymbol{PSM}}}\ (\text{PSM}) \end{cases} \tag{4}$$

where **Σ**, **U**, $\boldsymbol{\Sigma}_{\boldsymbol{PSM}}$, and $\mathbf{U_{PSM}}$ are the outcomes of the SVD process applied to the covariance matrices. The SVD process is executed using a Python script [21]. The matrices **Σ** and **U** are of size 72 × 72, and the matrices $\boldsymbol{\Sigma}_{\boldsymbol{PSM}}$ and $\mathbf{U_{PSM}}$ are of size 10,000 × 10,000. The matrices **A** and $\mathbf{A_{PSM}}$ are utilized in the STREAM perturbation process. To decrease the loading time of the $\mathbf{A_{PSM}}$ matrix, the HDF5 file format is employed. Equation (5) implemented in STREAM to perturb the cross-sectional data with EQ 2-term resonance treatment and PSM resonance treatment [16,22]. Matrix **A** and $\mathbf{A_{psm}}$ are calculated by SVD of covariance matrices [23]. To reduce the reading time of $\mathbf{A_{PSM}}$ matrix, HDF5 [24] file format is used.

$$\begin{cases} \boldsymbol{x}=\boldsymbol{A}\cdot\boldsymbol{z}+\boldsymbol{\mu}\ (\text{EQ 2}-\text{term}) \\ \boldsymbol{x}=\boldsymbol{A}_{\boldsymbol{PSM}}\cdot\boldsymbol{z}+\boldsymbol{\mu}\ (\text{PSM}) \end{cases} \tag{5}$$

where $\boldsymbol{z}$ is a matrix containing the standard normal random numbers, and $\boldsymbol{\mu}$ contains the mean variable [22,24]. Notation of $\boldsymbol{x}$ is perturbed cross-section data. The yellow section indicates the perturbation process in STREAM. To address the occurrence of negative cross sections during the perturbation process, a zero-cutoff option was applied, in line with previous UQ studies [25,26]. The Latin Hypercube Sampling (LHS) method was employed to generate random numbers with Box-Muller transform denoted as Equation (6) [9,10,27].

$$\begin{cases} z_1=\sqrt{-2\ln\xi_1}\sin(2\pi\xi_2) \\ z_2=\sqrt{-2\ln\xi_1}\cos(2\pi\xi_2) \end{cases} \tag{6}$$

where the z_1 and z_2 are random numbers conforming to the normal distribution, while ξ_1 and ξ_2 are random numbers following a uniform distribution within the range of 0–1. Fig. 1 presents the detailed progress of the UQ. The fission spectrum was normalized after the perturbation process [16]. Generation progress of covariance library has been verified with Los Alamos National Lab (LANL) results with comparable accuracy [16,28].

To assess the capability of the covariance library generation method

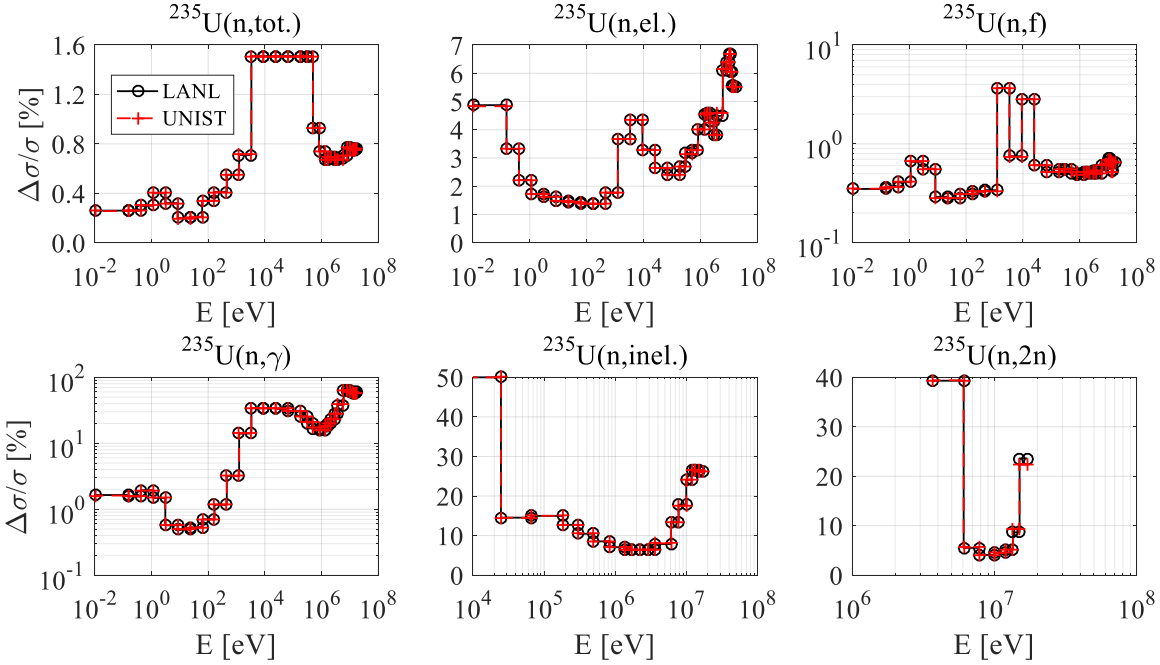

Fig. 2. Cross-section uncertainty ($\Delta\sigma/\sigma$) of ^{235}U as a function of energy.

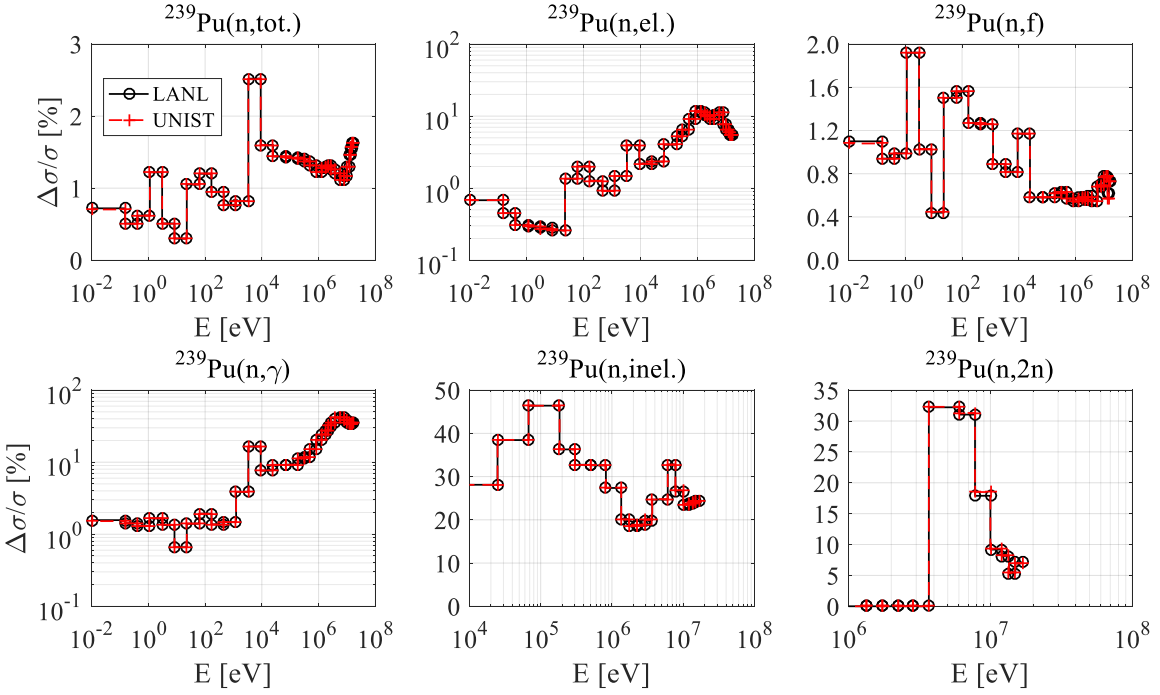

Fig. 3. Cross-section uncertainty ($\Delta\sigma/\sigma$) of ^{239}Pu as a function of energy.

used in this study, a comparison was made with a covariance library generated by LANL [29]. Figs. 2 and 3 show the relative differences in isotope uncertainty between this study (UNIST) and LANL [29]. For comparison, main isotopes that contribute significantly to uncertainty were selected: ^{235}U at the initial state and ^{239}Pu in the case of generated fissile material. The notations (n, tot.), (n, inel.), (n, f), (n, γ), (n, 2n), and (n, el.) represent the total cross-section, inelastic scattering cross-section, fission cross-section, capture cross-section, production of two neutrons, and elastic scattering cross-section, respectively. These figures demonstrate that the covariance library generated in this study has comparable accuracy to the LANL data.

2.2. PCA method

This section presents the PCA method for data compression. PCA operates as a compression methodology grounded in linear algebra, as

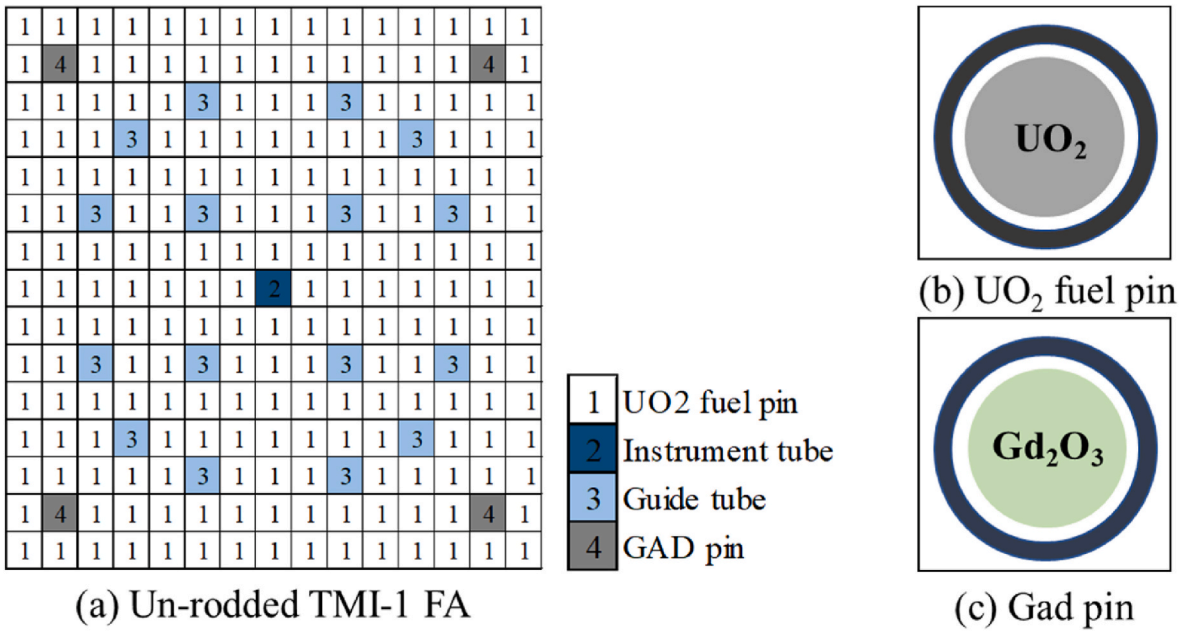

Fig. 4. Radial configuration of the TMI-1 FA and pin cell model.

Table 3
Specification of TMI-1.

Parameter	Value	Unit	Parameter	Value	Unit
Number of fuel rod	208		Fuel temperature	900	K
Number of guide tube	16		Moderator temperature	562	K
FA pitch	21.811	cm	Boron concentration	0	ppm
Pin pitch	1.4427	cm	Fuel radius	0.46950	cm
Number of Instrument tube	1		Air gap outer radius	0.47880	cm
Cladding outer radius	0.54610	cm	Instrument tube inner radius	0.56005	cm
Guide tube inner radius	0.63245	cm	Instrument tube outer radius	0.62610	cm
Guide tube outer radius	0.67310	cm	FA dimensions	15 × 15	

Table 4
HZP and HFP conditions for TMI-1 benchmark calculation.

	HFP	HZP
Fuel temperature [K]	900	551
Moderator temperature [K]	562	551
Boron concentration [ppm]	0	0

Table 5
Multiplication factor summary of TMI-1 benchmark calculation with scale 6.2 covariance library.

Code	SCALE 6.2.2, 252G		SCALE 6.2.2, 56G		STREAM, 72G	
Condition	$\overline{keff}$[a]	△k/k [%]	$\overline{keff}$	△k/k [%]	$\overline{keff}$	△k/k [%]
HFP	1.40979	0.5472	1.41088	0.5564	1.40954	0.5520
HZP	1.42811	0.5392	1.42936	0.5471	1.42810	0.5393

[a] Average of 500 perturbed keff.

depicted in the process flowchart shown in Fig. 1. Compression activity occurred between the STORA and RAST-K calculations. Specifically, the compression process involved three main steps: (1) data file compression using PCA, (2) application of the HDF5 format, and (3) utilization of

Table 6
TMI Pin cell (△k/k [%]) with SCALE 6.2 covariance library.

Code	HFP			HZP		
	SCALE 6.2.2		STREAM	SCALE 6.2.2		STREAM
Group	252G	56G	72G	252G	56G	72G
Reaction						
^{235}U (ν)	0.3405	0.3404	0.3404	0.3418	0.3417	0.3417
^{238}U (n, γ)	0.2821	0.2950	0.2904	0.2723	0.2834	0.2778
^{235}U (n, γ)	0.1964	0.1962	0.1945	0.1960	0.1959	0.1941
^{235}U (χ)	0.1558	0.1617	0.1540	0.1497	0.1556	0.1477
^{238}U (n, n')	0.1173	0.1186	0.1196	0.1103	0.1115	0.1125
^{235}U (n, f)	0.0766	0.0764	0.0792	0.0768	0.0766	0.0792
^{238}U (ν)	0.0713	0.0716	0.0696	0.0694	0.0697	0.0677
^{235}U (n, n')	0.0014	0.0014	0.0015	0.0013	0.0013	0.0014

the xz format. Truncated SVD is used for PCA. The recovered matrix, denoted as $\mathbf{B_{recover}}$, is defined as the product of matrices, **V**, **PC**, and **mu** added to matrix **Z**, as indicated in Equation (7) [16]. The matrix sizes of **V**, **PC**, **mu**, and **Z** are defined as $N_{sample} \times N_{PC}$, $N_{PC} \times N_{PC}$, $1 \times N_{PC}$, and $N_{sample} \times N_{z\_profile\_parameter}$, respectively. Here, N_{PC} represents the number of principal components (PCs), and N_{sample} is the number of perturbed samples. N_{PC} denotes the number of few-group constants generated by STREAM in one burnup step, which is defined as 444 for cross-section data at a specific burnup step. The **Z** profile matrix is defined as a sparse matrix, as it contains only $N_{z\_profile\_parameter}$ elements of N_{PC}. This approach is adopted to save memory, given that the matrix includes only a small number of elements. This $\mathbf{B_{recover}}$ is used for decompression progress [16].

$$\mathbf{B_{recover}} = \mathbf{V} \times \mathbf{PC} + \mathbf{mu} + \mathbf{Z} \tag{7}$$

where **V** is the reduced matrix and **PC** is a matrix that contains the principal components, with the default option being 30 in this study [16]. Matrix **mu** is the average matrix of original matrix **B** [16]. Matrix **Z** is the zero profile and has been developed to reduce the calculation error [16]. The decompression process takes only a few seconds, which means the time required for decompression can be considered negligibly small. The ramifications of such data loss on the UQ are assessed in Section 4.3, where verification is performed using the TMI-1 benchmark.

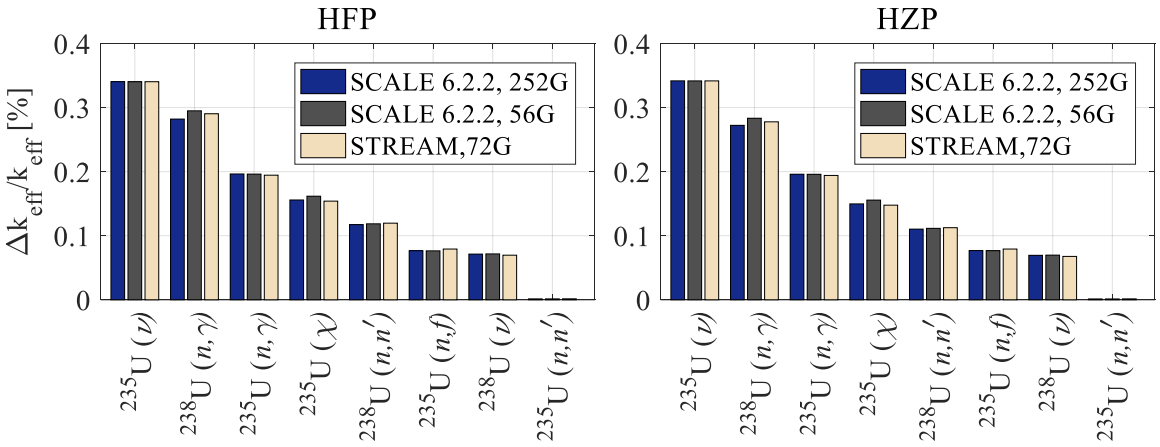

Fig. 5. Uncertainty of eight reactions with TMI-1 pin cell, scale 6.2 covariance data (56 group data).

Table 7
Summary of TMI-1 pin and FA results with ENDF/B-VII.1 covariance library.

Calculation model	Calculation condition	EQ 2-term		PSM	
		$\overline{keff}$*	△k/k [%]	$\overline{keff}$	△k/k [%]
Pin	HFP	1.41043	0.7550	1.41356	0.7507
	HZP	1.42909	0.7484	1.43183	0.7434
FA	HFP	1.39747	0.7329	1.40080	0.7285
	HZP	1.41386	0.7304	1.41676	0.7250

* $\overline{keff}$ is average of 500 perturbed keff.

Table 8
TMI-1 pin (△k/k [%]) with ENDF/B-VII.1 covariance library.

Condition	HFP		HZP	
Case Reaction	PSM	EQ 2-term	PSM	EQ 2-term
^{235}U (ν)	0.6062	0.6066	0.6087	0.6092
^{238}U (n, γ)	0.2986	0.2924	0.2830	0.2802
^{235}U (n, γ)	0.1854	0.1900	0.1887	0.1895
^{235}U (χ)	0.1681	0.1688	0.1641	0.1618
^{238}U (n, n')	0.1241	0.1247	0.1168	0.1172
^{235}U (n, f)	0.0726	0.0768	0.0720	0.0770
^{238}U (ν)	0.0729	0.0731	0.0710	0.0711

Table 9
TMI-1 FA (△k/k [%]) with ENDF/B-VII.1 covariance library.

Condition	HFP		HZP	
Case Reaction	PSM	EQ 2-term	PSM	EQ 2-term
^{235}U (ν)	0.6304	0.6309	0.6328	0.6333
^{238}U (n, γ)	0.2720	0.2710	0.2576	0.2599
^{235}U (n, γ)	0.1896	0.1919	0.1893	0.1919
^{235}U (χ)	0.1507	0.1514	0.1449	0.1455
^{238}U (n, n')	0.1040	0.1045	0.0981	0.0986
^{235}U (n, f)	0.0759	0.0815	0.0771	0.0816
^{238}U (ν)	0.0616	0.0617	0.0600	0.0601

3. Description of benchmark problems

This section provides detailed specifications for the TMI-1 benchmarks, as referenced in Refs. [1,30]. Fig. 4 shows the layout of the TMI-1 Fuel Assembly (FA) and the individual pin layouts. Subplot (a) presents the un-rodded TMI-1 FA model, while subplots (b) and (c) show the UO_2 fuel and gadolinia pins, respectively. Both the models were used for the calculations. The comprehensive geometric details are presented in Table 3 [30].

In the verification phase of the perturbation module integrated into STREAM, the TMI-1 pin model serves as a comparative baseline against SCALE 6.2.2, as discussed in Section 4.1. To validate the PSM covariance library within STREAM, calculations were conducted using both the pin and FA models, as described in Section 4.2. These calculations utilized the ENDF/B-VII.1 covariance library, and the outcomes were compared with those obtained via both EQ 2-term and PSM methodologies. During the evaluation of PCA in UQ, the FA model was specifically used, with additional details provided in Section 4.3.

4. Results and discussion

This section presents the calculation results obtained using the TMI-1 benchmark. Section 4.1 focuses on verifying the newly developed perturbation module by comparing it with SCALE 6.2.2, which is widely acknowledged for its utility in analyzing neutronic data uncertainties within the UAM benchmark [31–35] and serves as the reference for a code-to-code comparison. During this verification process, the UQ module integrated into STREAM uses TSUNAMI [36] as its counterpart in the SCALE 6.2.2. TSUNAMI computes uncertainties based on the Generalized Perturbation Theory [7]. For the calculations, 500 perturbed cross-sectional datasets were used to consult the previous studies [9,10,37]. STREAM utilizes a stochastic sampling method and leverages the ENDF/B-VII.1 neutronics library [8] along with the SCALE 6.2 covariance library [7].

Sections 4.2 and 4.3 are predicated the prediction using the ENDF/B-VII.1 covariance library. Section 4.2 presents the verification of the UQ module incorporating PSM, which was conducted in parallel with EQ 2-term calculation module. In Section 4.3, the computational efficiency of PCA in UQ is examined in the context of a two-step method. During verification, the computational efficacy of the two-step method was evaluated by juxtaposition with the UQ module of STREAM.

4.1. Verification of UQ module with SCALE 6.2.2 and SCALE 6.2 covariance library

This section outlines the verification process for the newly developed UQ calculation scheme using the TMI-1 benchmark as a standard. The verification involved a code-to-code comparison with the widely-used SCALE 6.2.2 software. This paper specifically focusses on calculations based on the TMI-1 UO_2 pin-cell model under two distinct operational conditions: Hot Zero Power (HZP) and Hot Full Power (HFP). The detailed parameters of these conditions are listed in Table 4.

Eight nuclear reactions were considered in these calculations. These reactions include nu-bar (ν), capture cross-section (n, γ), fission

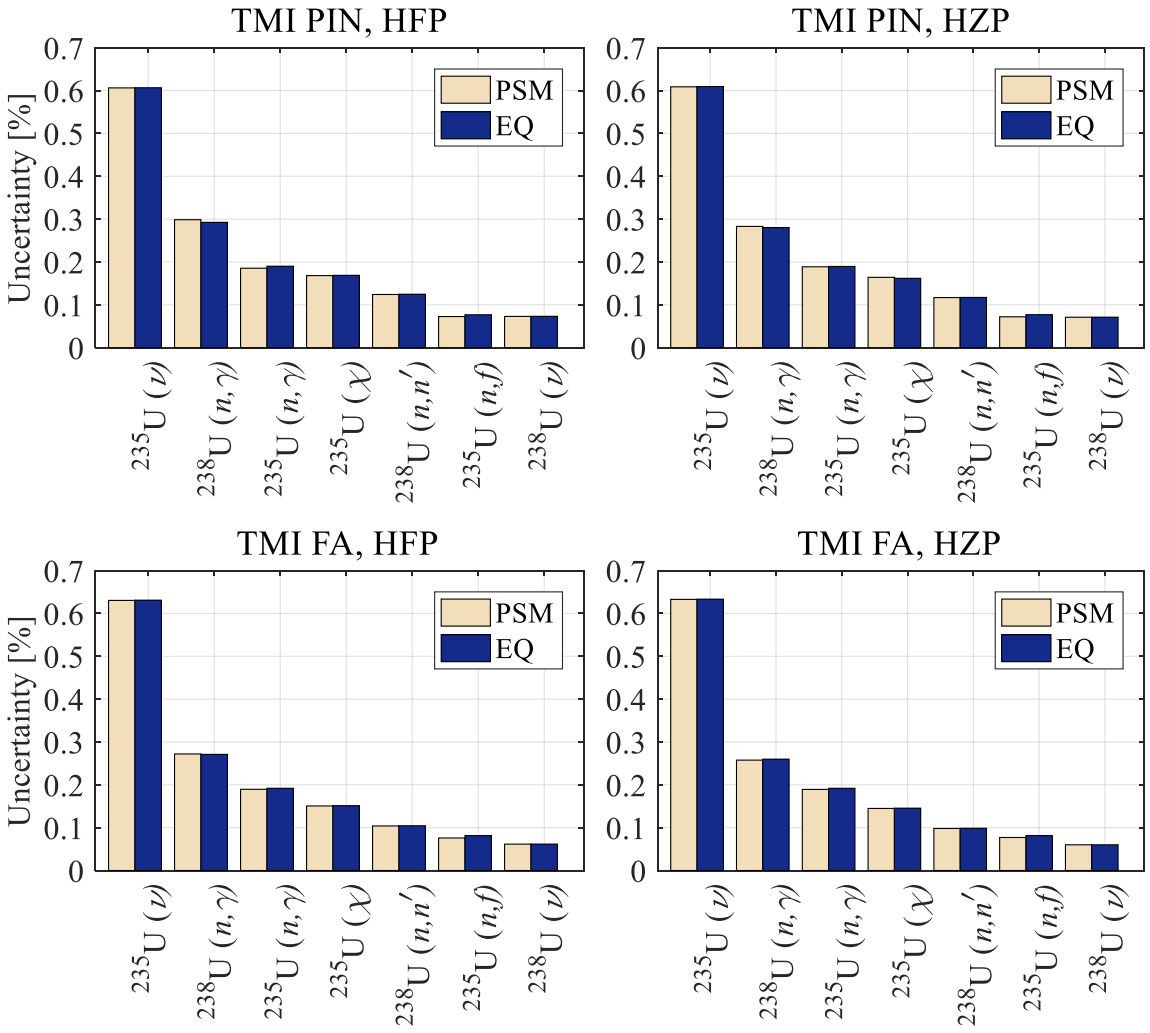

Fig. 6. Uncertainty compared with PSM and EQ 2-term resonance treatment, ENDF/B-VII.1 covariance library.

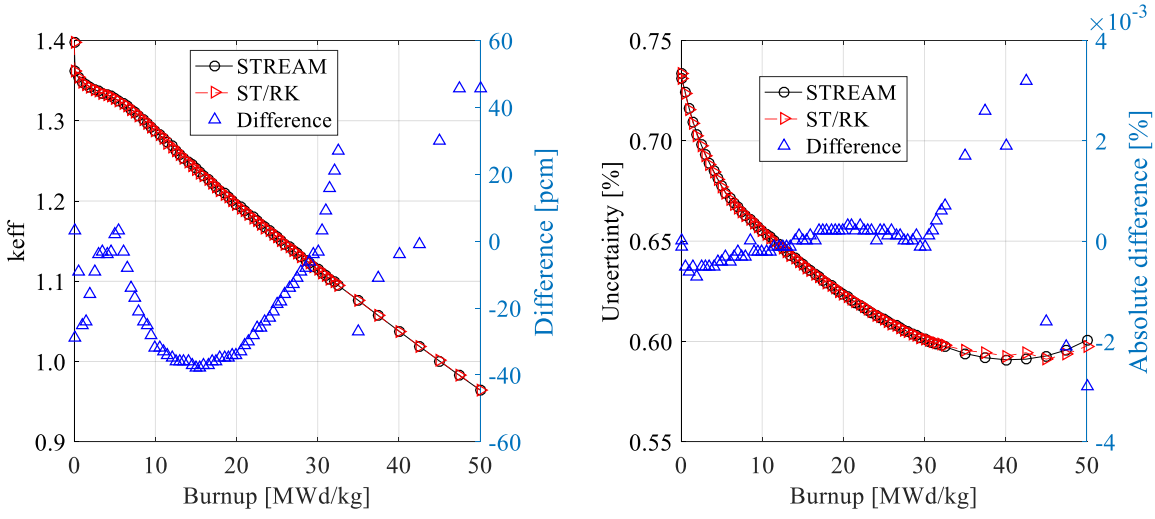

Fig. 7. Verification of the ST/RK results compared with STREAM.

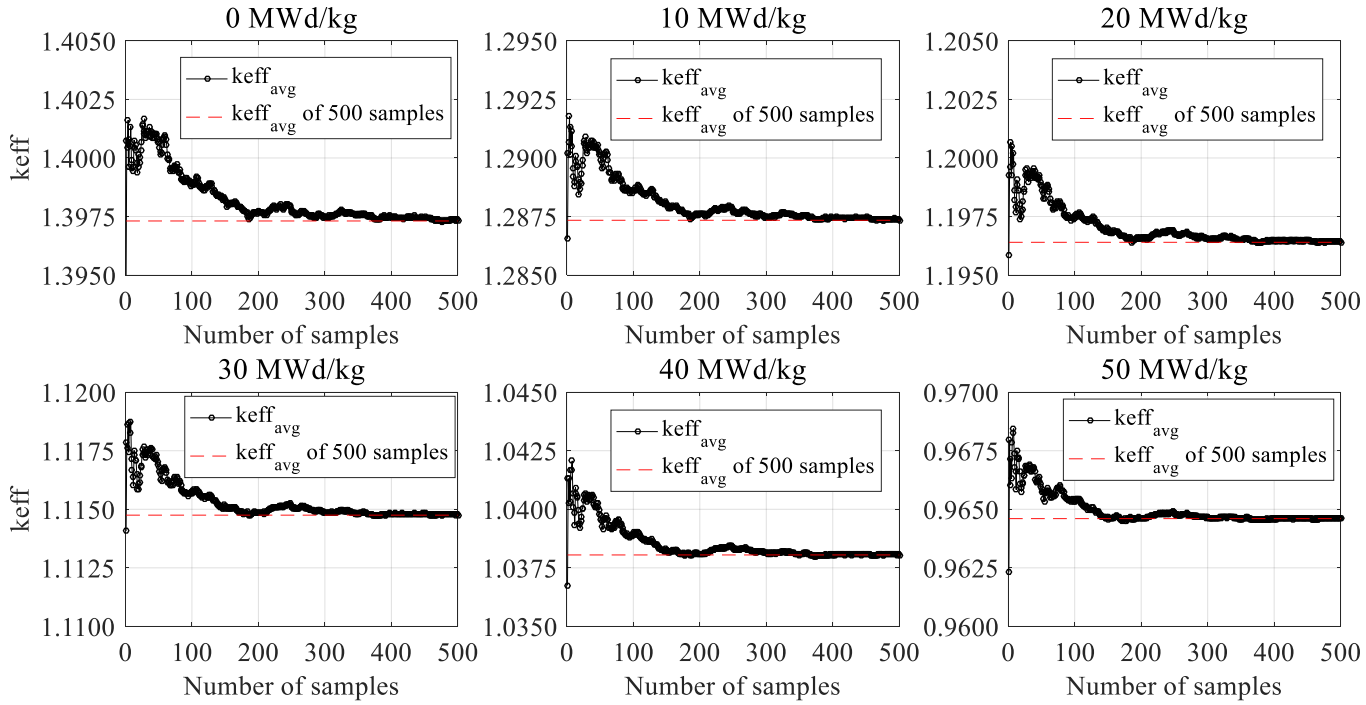

Fig. 8. Average of the samples with TMI-1 benchmark.

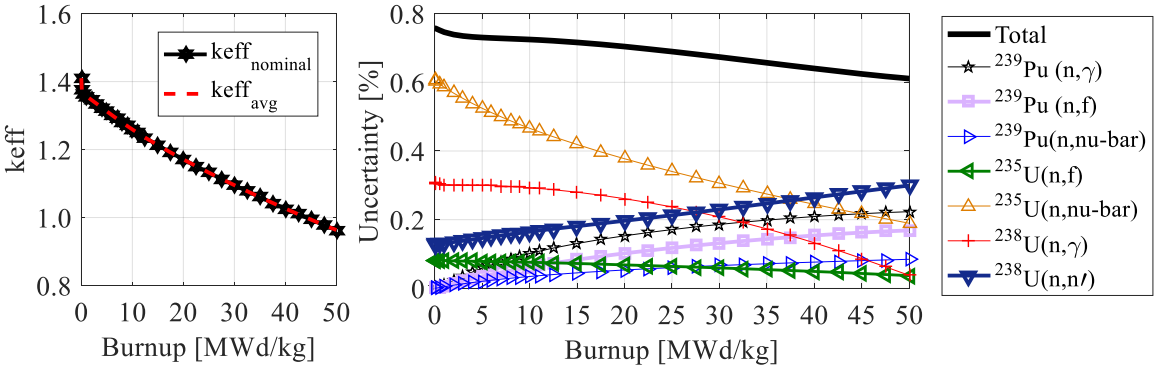

Fig. 9. Depletion as a function of burnup.

Table 10
Data compression efficiency (memory).

Case		Common	PC 30			PC 50		
Compression step		1	2	3	4	2	3	4
Method		Nominal	PCA (n = 30)	HDF5	xz	PCA (n = 50)	HDF5	xz
Memory [MB]	V	1450	71.232	42.739	25.644	118.72	71.232	42.739
	PC		63.812	38.287	22.972	105.364	63.218	37.931
	mu		2.968	1.781	1.068	2.968	1.781	1.068
	Z		146.916	88.150	52.890	146.916	88.150	52.890
	Total	1450	284.928	170.957	102.5741	373.968	224.381	134.629
Compression ratio [%]		0	80.350	88.210[a]	92.926[b]	74.209	84.525[a]	90.715[b]

a mode provides the on-the-fly calculation; *b* mode provides just for save the parameters.

spectrum (χ), inelastic scattering (n, n'), and fission cross-section (n, f). Table 4 lists the uncertainties attributed to each reaction. For example, the uncertainty for the ^{235}U (ν) reaction is determined through ν perturbation alone, without considering the perturbations of the other 13 reactions listed in Table 1. The uncertainty is quantified as the ratio of the absolute uncertainty to the multiplication factor.

For comparison, two different group structures from SCALE 6.2.2 are considered: a 252-group (252G) and a 56-group (56G) case are considered. The calculations employed the ENDF/B-VII.1, xn252v7.1, and xn56v7.1, libraries that were specifically used for the 252G and 56G cases, respectively. By contrast, STREAM employs a 72-group (72G) structure from the same ENDF/B-VII.1 library and applies EQ 2-term

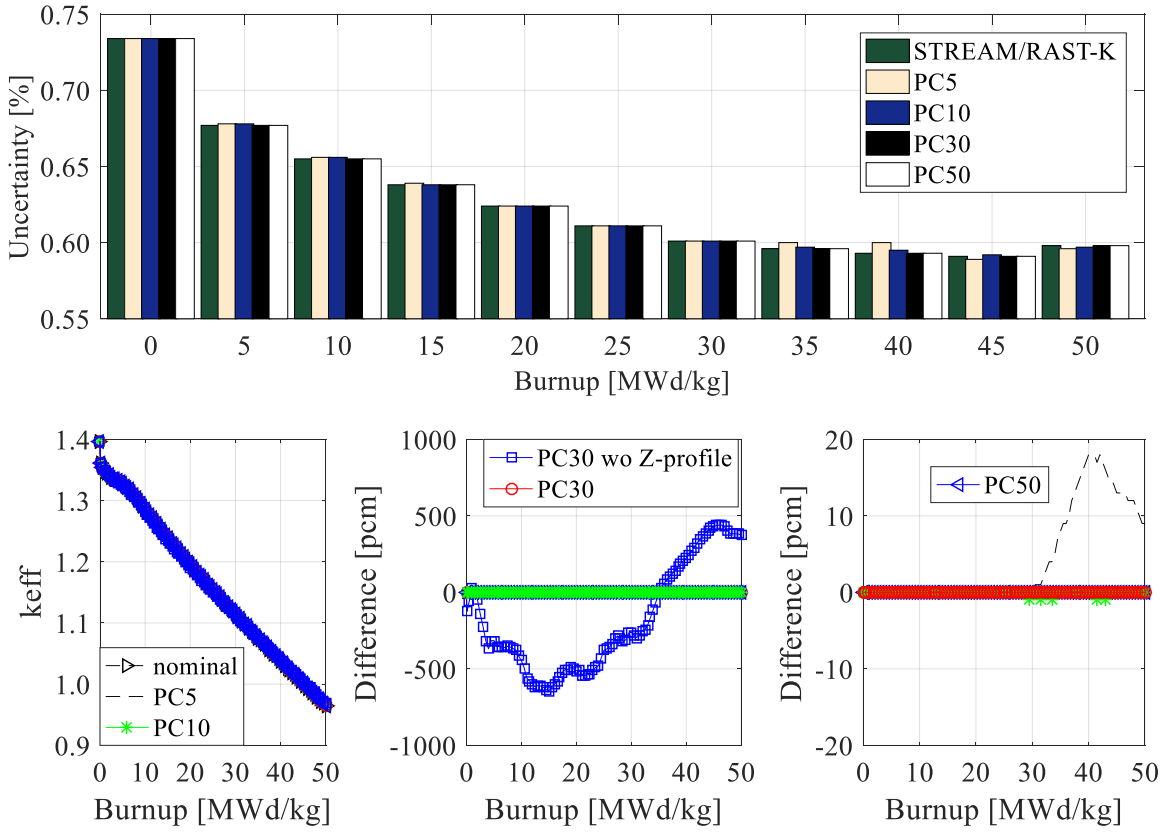

Fig. 10. Uncertainty and multiplication factor as a function of burnup.

method for resonance treatment.

As demonstrated in Table 5 and Table 6, both the multiplication factors and uncertainties calculated using STREAM were in close agreement with those obtained from SCALE 6.2.2. Fig. 5 graphically represents the uncertainties for the eight reactions calculated using both STREAM and SCALE 6.2.2. Notably, the results from STREAM aligned closely with those from SCALE 6.2.2 252G.

4.2. Verification of PSM covariance library

This section elaborates the verification of the newly implemented UQ module, which incorporates a PSM covariance library, setting it against the previously verified EQ 2-term method. EQ 2-term method serves as a reference point for the code-to-code comparison, and its verification is discussed in Section 4.1. ENDF/B-VII.1 covariance library is used for these calculations. A summary of the averaged effective multiplication factors (keff) calculated from the perturbed cross-sectional data, along with the associated uncertainties, is provided in Table 7. The calculations were conducted under both HFP and HZP conditions, with additional details outlined in Table 4. Two different models, the UO_2 fuel pin cell and the FA, formed the basis for these calculations. The corresponding results are displayed in Table 8, Table 9 and Fig. 6. As evidenced by the data in these tables and the figure, the accuracy levels achieved with the PSM method are on par with those achieved with EQ 2-term method.

4.3. Verification of PCA method in STREAM/RAST-K UQ with TMI-1

This section discusses the computational efficiency and validation of the data compression techniques used in the UQ of the STREAM/RAST-K two-step method. Specifically, the lossless compression methods HDF5 and xz, along with the lossy PCA method, were employed. This section focuses on the results of the depletion calculations.

To evaluate the computational performance of the STREAM/RAST-K two-step method in the UQ calculations, verification was conducted using STREAM as a reference. In the two-step approach, RAST-K uses perturbed cross-sectional data generated by STREAM. Fig. 7 shows the verification results. The calculation conditions included a fuel temperature of 900 K, a moderator temperature of 562 K, and a boron concentration of 0.2 ppm. A MOC ray with a 0.03 cm track spacing was employed in STREAM. The TMI-1 FA model was used as the basis for these calculations. As the burnup proceeded, the average multiplication factors and associated uncertainties were compared. The differences in these factors were within 46 pcm between STREAM and STREAM/RAST-K (ST/RK) throughout the entire depletion range, with uncertainty variations confined to 0.032%. The results indicate that STREAM/RAST-K achieved an accuracy comparable to that of STREAM alone. In total, 500 calculation samples were considered.

For convergence analysis, Fig. 8 compares the average multiplication factors of the perturbed samples calculated using STREAM. The Shapiro-Wilk test was used to determine whether the calculated samples were normally distributed [38]. The p-values for these samples exceed 0.05 across all burnup levels, suggesting a normal distribution across all burnup levels. Fig. 9 plots the uncertainties as functions of the burnup calculated using the STREAM/RAST-K two-step method. The 'Total' case refers to the calculation scenario in which all perturbed cross-section data are used to estimate uncertainty as a function of burnup. The isotope and reaction selections were guided by a previous [39]. This figure also depicts the results for the seven most influential reactions, detailing their behavior over the burnup course. The uncertainty trends aligned well with those of previous UQ studies.

Table 10 lists the data compression ratios attained through PCA, HDF5, and xz methods. For on-the-fly calculations, the compression ratio reaches 88.210% in the 30 PC case and 84.525% in the 50 PC case.

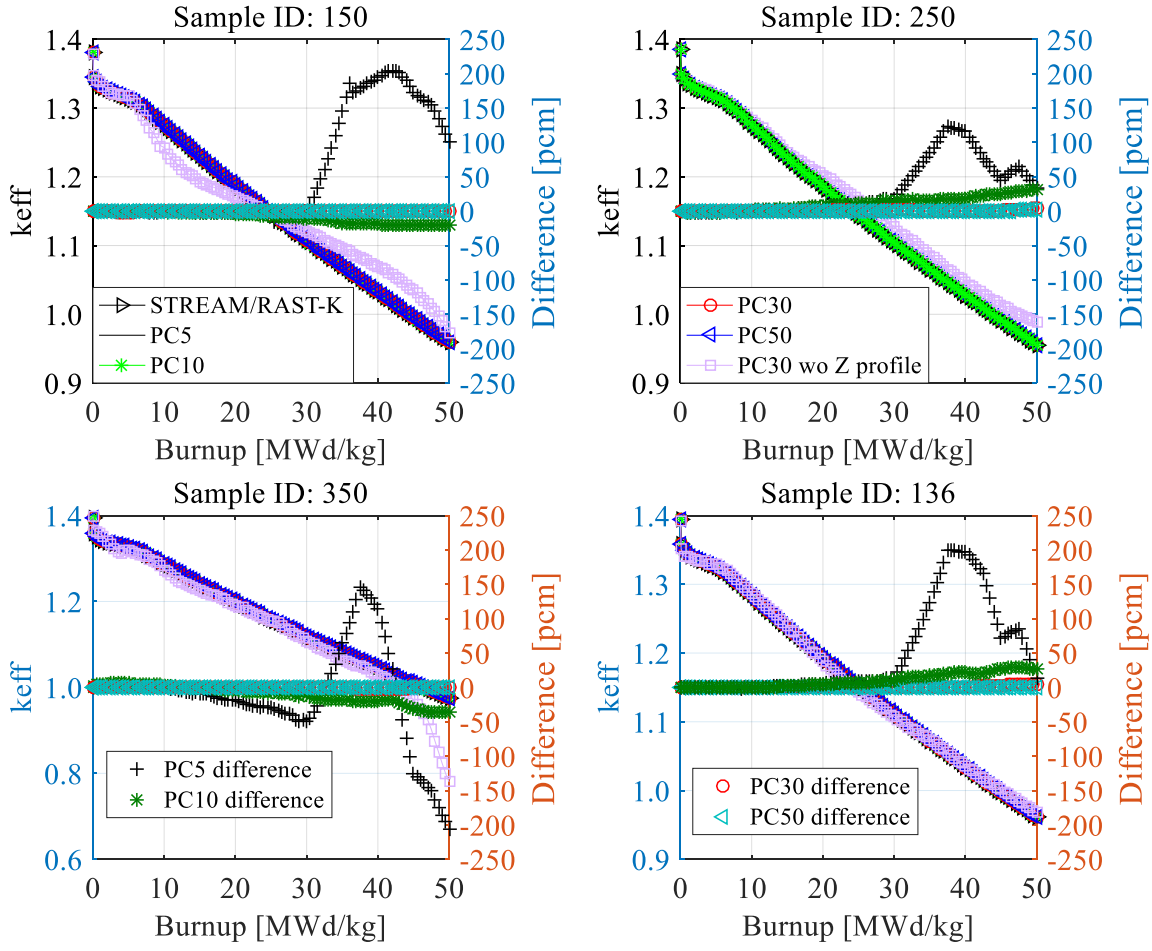

Fig. 11. keff with PCA (sensitivity study results) – PC and Z profile check.

For the 30 PC case, the matrix sizes are defined as follows: **V** is 500 × 30, **PC** is 30 × 444, mu is 1 × 444, and **Z** is 500 × 62. During this calculation, 62 elements selected for inclusion in the z-profile file undergo a sensitivity study. For the 50 PC case, the matrix sizes of **V** and **PC**, which are related to the number of principal components, differ: **V** is 500 × 50 and **PC** is 50 × 444. When saving the data files, these ratios stand at 92.926% and 90.715%, respectively. The compression ratio is determined using Equation (8).

$$\text{Compression ratio} = \left(1 - \frac{\textit{memory of compressed data file}}{\textit{memory of nominal data file}}\right) * 100\ [\%] \tag{8}$$

This represents the method for compressing the data file compared to the nominal data file. As demonstrated in a previous study [5], the number of principal components has a significant relationship with the total memory, and 30 principal components were used for the calculation. The calculation using 30 principal components resulted in truncation errors within 0.01% of the radial power distribution. Moreover, the multiplication factor was compared in this calculation, and a scale order of 10^{-5} was essential for the comparison of multiplication factors. Therefore, to achieve high accuracy in the calculations, a z-profile data file was used, which included 62 variables related to $^{234\text{-}236}$U, ^{238}U, $^{237\text{-}239}$Np, $^{239\text{-}242}$Pu, $^{241\text{ and }243}$Am, and ^{244}Cm. These isotopes contribute significantly to the calculation of the multiplication factor and require a large memory compared to a previous study [5]. Consequently, the compression ratio was slightly lower than that reported in a previous study [5], reaching 92.926%. An additional xz file format is used to save the files. An xz file has the advantage of high accuracy because it is lossless [11]. However, the x–z method does not support on-the-fly calculations. Therefore, PCA and HDF5 data compression methods were used for on-the-fly calculations.

Figs. 10 and 11 show the detailed results. Fig. 10 shows the results of a sensitivity study that varied the number of PCs used in the PCA. For these calculations, 500 perturbed samples are evaluated using the ENDF/B-VII.1 covariance library. We compared five distinct scenarios using 5, 10, 30, and 50 PCs along with z-profile data, as well as a case using 30 PCs without z-profile data. As indicated in Fig. 10, the scenario omitting the z-profile data showed a discrepancy greater than 500 pcm, thus underlining the importance of the z-profile data for achieving computational accuracy. When comparing the various PC scenarios, both the 30 PC and 50 PC cases produce results with high accuracy, showing errors within ±1 pcm and 0 pcm over the entire depletion range, respectively. Additionally, these cases closely aligned with the nominal calculations in terms of uncertainty. Fig. 11 delves deeper into the comparison and features four specific perturbed sample cases: the 150th, 250th, 350th, and 136th. The results demonstrate that both the 30 PC and 50 PC scenarios yield highly accurate outcomes when compared to the nominal calculations, with differences within ±5 pcm and ±2 pcm, respectively. In stark contrast, the scenario without the z-profile data showed deviations exceeding 500 pcm, further underscoring the necessity for accurate calculations. Upon examining the data presented in Table 10, Figs. 10 and 11, it is evident that the 30 PC scenario

optimizes the balance between memory efficiency and computational accuracy.

5. Conclusion

This study paper introduces an uncertainty analysis of the TMI-1 benchmark using the STREAM/RAST-K two-step method. The study presents two significant advancements: (1) Development of an UQ module and the creation of covariance library for PSM resonance treatment. (2) Application of PCA for UQ. To validate the calculation module, the TMI-1 benchmark is employed. The analysis includes 500 perturbed samples and utilizes ENDF/B-VII.1 neutronics data in conjunction with both ENDF/B-VII.1 and SCALE 6.2.2 covariance libraries. When compared to SCALE 6.2.2, the STREAM method demonstrates comparable accuracy, with discrepancies as small as ±0.0078% for both Hot Full Power (HFP) and Hot Zero Power (HZP) pin cell model calculations. These calculations are performed for both the 252-group and 56-group scenarios. The PSM covariance library is generated using various tools, including NJOY-2016, NJOYCOVX, CADILLAC, and COGNAL. Compared to EQ 2-term calculation module, our newly developed PSM module shows a marginal difference of ±0.0054% in both HFP and HZP pin cell and FA model calculations when using the ENDF/B-VII.1 covariance library. Furthermore, we validate PCA by applying it to TMI-1 FA models. The compression scheme employed achieves compression ratios of 88.210% and 92.926% for the on-the-fly and data-saving methods, respectively.

In summary, this study paper contributes to the field by providing an uncertainty analysis of the TMI-1 benchmark, a significant component of the UAM benchmarks. Future research will aim to extend uncertainty quantification (UQ) analyses to include implicit effects and will also explore the impact of memory compression using the PCA method in deterministic UQ.

Declaration of competing interest

The authors declare that they have no known competing financial interests or personal relationships that could have appeared to influence the work reported in this paper.

Acknowledgments

This work was supported by the National Research Foundation of Korea (NRF) grant funded by the Korea government (MSIT). (No. NRF-2019M2D2A1A03058371).

Abbreviations

CRAM	Chebyshev rational approximation method
EQ 2-term	Calvik's two-term rational approximation
FA	fuel assembly
HFP	hot full power
HZP	hot zero power
MOC	Method of Characteristics
PC	principal component
PCA	principal component analysis
PSM	pin-based pointwise energy slowing-down method
SVD	singular value decomposition
UAM	uncertainty analysis in modeling
UQ	uncertainty quantification

References

[1] R.N. Bratton, M. Avramova, K. Ivanov, OECD/NEA benchmark for uncertainty analysis in modeling (UAM) for LWRS – summary and discussion of neutronics cases (phase I), Nucl. Eng. Technol. 46 (2014) 313–342, https://doi.org/10.5516/NET.01.2014.710. Organization for Economic Co-operation and Development.

[2] S. Choi, W. Kim, J. Choe, W. Lee, H. Kim, B. Ebiwonjumi, E. Jeong, K. Kim, D. Yun, H. Lee, D. Lee, Development of high-fidelity neutron transport code STREAM, Comput. Phys. Commun. 264 (2021), https://doi.org/10.1016/j.cpc.2021.107915.

[3] J. Park, J. Jang, H. Kim, J. Choe, D. Yun, P. Zhang, A. Cherezov, D. Lee, RAST-K v2—three-dimensional nodal diffusion code for pressurized water reactor core analysis, Energies 13 (2020) 6324, https://doi.org/10.3390/en13236324.

[4] S. Choi, C. Lee, D. Lee, Resonance treatment using pin-based pointwise energy slowing-down method, J. Comp. Physiol. 330 (2017) 134–155, https://doi.org/10.1016/j.jcp.2016.11.007.

[5] A. Cherezov, J. Jang, D. Lee, A PCA compression method for reactor core transient multiphysics simulation, Prog. Nucl. Energy 128 (2020), https://doi.org/10.1016/j.pnucene.2020.103441.

[6] I.T. Jolliffe, J. Cadima, Principal component analysis: a review and recent developments, Philos. Trans. A Math. Phys. Eng. Sci. 374 (2016), 20150202, https://doi.org/10.1098/rsta.2015.0202.

[7] B.T. Rearden, M.A. Jessee, Scale Code System, Oak Ridge National Laboratory, 2017.

[8] M.B. Chadwick, M. Herman, P. Obložinský, M.E. Dunn, Y. Danon, A.C. Kahler, D. L. Smith, B. Pritychenko, G. Arbanas, R. Arcilla, R. Brewer, D.A. Brown, R. Capote, A.D. Carlson, Y.S. Cho, H. Derrien, K. Guber, G.M. Hale, S. Hoblit, S. Holloway, T. D. Johnson, T. Kawano, B.C. Kiedrowski, H. Kim, S. Kunieda, N.M. Larson, L. Leal, J.P. Lestone, R.C. Little, E.A. McCutchan, R.E. MacFarlane, M. MacInnes, C. M. Mattoon, R.D. McKnight, S.F. Mughabghab, G.P.A. Nobre, G. Palmiotti, A. Palumbo, M.T. Pigni, V.G. Pronyaev, R.O. Sayer, A.A. Sonzogni, N.C. Summers, P. Talou, I.J. Thompson, A. Trkov, R.L. Vogt, S.C. van der Marck, A. Wallner, M. C. White, D. Wiarda, P.G. Young, ENDF/B-VII.1 nuclear data for science and technology: cross sections, covariances, fission product yields and decay data, Nucl. Data Sheets 112 (2011) 2887–2996, https://doi.org/10.1016/j.nds.2011.11.002.

[9] J. Jang, C. Kong, B. Ebiwonjumi, Y. Jo, D. Lee, Uncertainties of PWR spent nuclear fuel isotope inventory for back-end cycle analysis with Stream/RAST-K, Ann. Nucl. Energy 158 (2021), https://doi.org/10.1016/j.anucene.2021.108267.

[10] J. Jang, C. Kong, B. Ebiwonjumi, A. Cherezov, Y. Jo, D. Lee, Uncertainty quantification in decay heat calculation of spent nuclear fuel by Stream/RAST-K, Nucl. Eng. Technol. 53 (2021) 2803–2815, https://doi.org/10.1016/j.net.2021.03.010.

[11] L. Collin, xz." [Online], http://tukaani.org/xz/xz-5.0.7.tar.gz.

[12] D. Tomatis, A. Dall'Osso, Compression of 3D pin-by-pin burnup data, Ann. Nucl. Energy 136 (2020), 107058, https://doi.org/10.1016/j.anucene.2019.107058.

[13] X. Wu, C. Wang T, Kozlowski, kriging-based surrogate models for uncertainty quantification and sensitivity analysis, M&C, Jeju, Korea (2017). April 16–20.

[14] R.J.J. Stamm'ler, M.J. Abbate, (LONDON) LTD, 1983, 0-12-663320-7.

[15] D. Knott, A. Yamamoto, Lattice physics computations, in: D.G. Cacuci (Ed.), Handbook of Nuclear Engineering, Springer, 2010, pp. 913–1239.

[16] J. Jang, Development of Nodal Diffusion Code for VVER and HTGR Analysis with Advanced Semi Analytic Nodal Method, Doctoral Thesis, Ulsan National Institute of Science and Technology, 2023.

[17] J. Choe, S. Choi, P. Zhang, J. Park, W. Kim, H.C. Shin, H.S. Lee, J. Jung, D. Lee, Verification and validation of Stream/RAST-K for PWR analysis, Nucl. Eng. Technol. 51 (2019) 356–368, https://doi.org/10.1016/j.net.2018.10.004.

[18] D.W. Muir, R.M. Boicourt, A.C. Kahler, J.L. Conlin, W. Haeck, The NJOY Nuclear Data Processing System, Version 2016, LA-UR-17-20093, Los Alamos National Laboratory, 2016.

[19] M. Herman, A. Trkov, ENDF-6 formats manual, data formats and procedures for the evaluated nuclear data files ENDF/B-VI and ENDF/B-VII, National nuclear data center, Brookhaven National Laboratory, CSEWG Document ENDF-102, Report BNL-90365 Rev 1 (2009) 2010.

[20] G. Chiba, ERRORJ: A Code to Process Neutron-Nuclide Reaction Cross Section Covariance, Japan Atomic Energy Agency, 2007 version 2.3, March.

[21] V.C. Klema, A.J. Laub, The singular value decomposition: its computation and some applications, IEEE Trans. Automat. Control 25 (2) (1980). https://ieeexplore.ieee.org/document/1102314.

[22] A. Yamamoto, K. Kinoshita, T. Watanabe, T. Endo, Y. Kodama, Y. Ohoka, T. Ushio, H. Nagano, Uncertainty quantification of LWR core characteristics using random sampling method, Nucl. Sci. Eng. 181 (2015) 160–174, https://doi.org/10.13182/NSE14-152.

[23] V.C. Klema, A.J. Laub, The singular value decomposition: its computation and some applications, IEEE Trans. Automat. Control 25 (1980). https://ieeexplore.ieee.org/document/1102314.

[24] HDF, User's guide HDF5, Release 1.10 (2019). The HDF Group, https://portal.hdfgroup.org/display/HDF5/HDF5+User+Guides?preview=/53610087/53610088/Users_Guide.pdf.

[25] T. Zhu, Sampling-Based Nuclear Data Uncertainty Quantification for Continuous Energy Monte Carlo Codes, École Polytechnique Fédérale de Lausanne, 2015, https://doi.org/10.5075/epfl-thesis-6598.

[26] N.J. Quartemont, A.A. Bickley, J.E. Bevins, Nuclear data covariance analysis in radiation-trransport simulations utilizing SCALE sampler and the IRDFF nuclear data library, IEEE Trans. Nucl. Sci. 67 (2020) 482–491.

[27] K.A. Kinoshita, T. Yamamoto, Y. Endo, Y. Kodama, T. Ohoka, H. Ushio, Nagano, Uncertainty Quantification of Nutronics Characteristics Using Latin HyperCube Sampling Method, September 28, PHYSOR, Japan, 2014. Kyoto.

[28] R.E. MacFarlane, Covariance plots for ENDF/B-VII.1. https://t2.lanl.gov/nis/data/endf/covVII.1/. Los Alamos National Laboratory.

[29] E. Robert, MacFarlane, covariance plots for ENDF/B-VII.1, los alamos national laboratory. https://t2.lanl.gov/nis/data/endf/covVII.1.

[30] K.M. Ivanov, S. Avramova, I. Kamerow, E. Kodeli, E. Sartori, O. Cabellos, Ivanov, Benchmark for Uncertainty Analysis in Modelling (Uam) for Design, Operation and Safety Analysis of LWRs, Volume I: Specification and Support Data for the Neutronics Cases (Phase I), OECD Nuclear Energy Agency, June 2016.
[31] E. Canuti, A. Petruzzi, F. D'Auria, T. Kozlowski, Sensitivity studies for the exercise I-1 of the OECD/UAM benchmark, 2012, Science and Technology of Nuclear Installations (2012) 10, https://doi.org/10.1155/2012/817185. pages article ID 817185.
[32] H.J. Park, McCARD/MIG stochastic sampling calculations for nuclear cross section sensitivity and uncertainty analysis, Nucl. Eng. Technol. 54 (2022) 4272–4279, https://doi.org/10.1016/j.net.2022.06.012.
[33] A. Labarile, N. Olmo, R. Miró, T. Barrachina, G. Verdú, Comparison of SERPENT and SCALE methodology for LWRs transport calculations and additionally uncertainty analysis for cross-section perturbation with SAMPLER module, EPJ Nuclear Sci. Technol. 2 (2016), https://doi.org/10.1051/epjn/e2016-50002-7.
[34] L. Mercatali, K. Ivanov, V.H. Sanchez, SCALE modeling of selected neutronics test problems within the OECD UAM LWR's benchmark, Sci. Technol. Nucl. Installations. (2013) 1–11, https://doi.org/10.1155/2013/573697, 2013.
[35] C. Arenas, R. Bratton, F. Reventos, K. Ivanov, Uncertainty analysis of light water reactor fuel lattices, Sci. Technol. Nucl. Installations (2013) 1–10, https://doi.org/10.1155/2013/437409, 2013.
[36] B.T. Rearden, M.L. Williams, M.A. Jessee, D.E. Mueller, D.A. Wiarda, Sensitivity and Uncertainty Analysis Capabilities and Data in SCALE, 174, 2011, https://doi.org/10.13182/NT174-236.
[37] G. Ilas, H. Liljenfeldt, Decay heat uncertainty for BWR used fuel due to modeling and nuclear data uncertainties, Nucl. Eng. Des. 319 (2017) 176e184, https://doi.org/10.1016/j.nucengdes.2017.05.009.
[38] NUREG, CR-6698, Guide for Validation of Nuclear Criticality Safety Calculational Methodology, Science Applications International Corporation, United States Nuclear Regulatory Commission, 2001.
[39] O. Leray, D. Rochman, P. Grimm, H. Ferroukhi, A. Vasiliev, M. Hursin, G. Perret, A. Pautz, Nuclear data uncertainty propagation on spent fuel nuclide compositions, Ann. Nucl. Energy 94 (2016) 603–611, https://doi.org/10.1016/j.anucene.2016.03.023.